

The quantum defect: The true measure of time-dependent density-functional results for atoms

Meta van Faassen^{a)} and Kieron Burke

Department of Chemistry and Chemical Biology, Rutgers University, Piscataway, New Jersey 08854-8087

(Received 11 November 2005; accepted 17 January 2006; published online 1 March 2006)

Quantum defect theory is applied to (time-dependent) density-functional calculations of Rydberg series for closed shell atoms: He, Be, and Ne. The performance and behavior of such calculations are much better quantified and understood in terms of the quantum defect rather than transition energies. © 2006 American Institute of Physics. [DOI: [10.1063/1.2173252](https://doi.org/10.1063/1.2173252)]

I. INTRODUCTION

Time-dependent density-functional theory¹ (TDDFT) has enjoyed a recent surge in popularity for calculating excited-state energies of atoms, molecules, clusters, and solids.^{2,3} TDDFT has features similar to ground-state density-functional theory (DFT): It produces useful accuracy at a fraction of the computational cost of *ab initio* methods,² but reliability depends on the approximate functionals used.⁴ As more and more practitioners in many subfields of computational science use TDDFT, there are ever increasing numbers of implementations. Calculations on atoms and sequences of atoms are often used to benchmark new implementations or to show how well TDDFT works in the simplest cases. These are particularly useful, as much highly accurate data, both from experiment and accurate wave function calculations, are available for these systems.

A well-known difficulty that hampered even the earliest calculations of excitations in atoms with TDDFT (Ref. 5) is the incorrect asymptotic behavior of the ground-state potentials of common density-functional approximations. It has long been known that the exact Kohn-Sham (KS) potential for a closed shell atom decays as $-1/r$ at large r , where r is the distance from the nucleus.^{6,7} Typical approximations for the ground state, such as the local density approximation (LDA), gradient corrected functionals (GGAs), and hybrid functionals (see, for example, Ref. 8 and references therein), have potentials that decay too rapidly with r . Only those with the correct asymptotic behavior support the Rydberg series of transitions, an infinite number of transitions that merge with the continuum at the ionization threshold. Orbital-dependent functionals capture this behavior naturally, as does the Van Leeuwen–Baerends potential approximation (LB94),⁹ which was designed to have an asymptotically correct behavior. Several recent methods have been suggested for correcting the standard functionals to produce the long-ranged tail.^{10–12} In any event, our present work applies only to long-ranged potentials.

We argue here that the way in which results have been calculated and reported for atoms is far from optimal. We show that long lists of transition frequencies for Rydberg

series converging to the ionization threshold are *not* the best way to report such calculations. Instead, the well-developed theory of the quantum defect¹³ is ideal for this purpose. Quantum defect theory has been used for decades in atomic physics (see, for example, Ref. 14 and references therein) and spectroscopy (see, for example, Ref. 15 and references therein). Quantum defect theory can also be applied to the class of Rydberg molecules,¹⁶ and some recent studies of molecular quantum defects with *ab initio* methods can be found in Refs. 17–19. In this paper we will only focus on atoms. One reason for this is the simple relation between excitation energies, which can be obtained from TDDFT, and the atomic quantum defect. Another reason is that we know the exact ground-state exchange-correlation (x_c) potential for some small atoms so we can compare any DFT results with the exact values.

We show that, for each Rydberg series, i.e., for each value of angular momentum l , two or three numbers completely characterize all the information in the infinite series. Furthermore, the quantum defect is a much more demanding test of excitation energies, and methods that appear to have only small energetic errors can yield quite poor quantum defect behavior. Also, shifts in orbital energies, such as the missing correlation contribution in the exact exchange highest occupied molecular orbital (HOMO) energy, have no effect on the quantum defect, so that the quality of a potential can be assessed without being influenced by such errors. We also find²⁰ that the quantum defect of the exact ground-state Kohn-Sham (KS) potential is sometimes, but not always, a good starting point for approximations to the true quantum defect.

II. THEORY

In Fig. 1 we show the orbital energy level diagram of the helium atom. The zero is set at the onset of the continuum, marked with a dotted line. For closed shell atoms and for any spherical one-electron potential that decays as $-1/r$ at large distances, the bound-state transitions form a Rydberg series with frequencies

^{a)}Electronic mail: faassen@rutchem.rutgers.edu

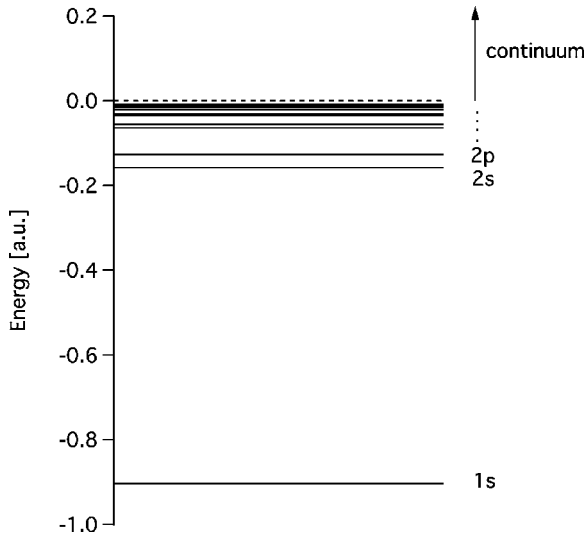
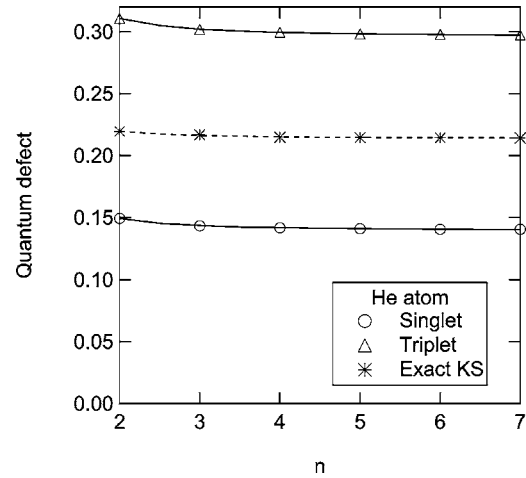


FIG. 1. Energy level diagram for the helium atom.

$$\omega_{nl} = I - \frac{1}{2(n - \mu_{nl})^2}, \quad (1)$$

where I is the ionization potential and μ_{nl} is called the quantum defect. We use atomic units ($e^2 = \hbar = m_e = 1$) throughout. The value of the quantum defect is that, for real atoms, quantum defects depend only weakly on the principle quantum number n for large n and converge to a finite value in the limit $n \rightarrow \infty$. In fact, according to Seaton's theorem,²¹ the quantum defect is a smooth function of energy as $E \rightarrow 0$ and merges continuously with the phase shift (relative to pure Coulomb scattering) divided by π . In Table I, we report extremely accurate results from wave function calculations for the helium atom. We show singlet and triplet values that have been obtained by Drake.²² We also give results from the exact ground-state KS potential, as found by Umrigar and Gonze.²³ We say more on how we obtained the KS values in Sec. III A. On the left are the transition frequencies while on the right are the corresponding quantum defects. Note how small the differences between transitions become as one climbs up the ladder, and yet the quantum defect remains finite and converges to a definite value.

In Fig. 2 we show the exact s KS quantum defect and the singlet and triplet quantum defects corresponding to accurate wave function results²² for helium as symbols. This is the

FIG. 2. The exact s KS quantum defect and the exact singlet and triplet quantum defects (Ref. 22) of He and their parabolic fits.

way the defect was plotted in Ref. 20 for the case of the Ne atom. However, it is more appropriate still to plot the defect as a function of energy, as shown in Fig. 3. This clearly illustrates that the quantum defect is a smooth function of energy and will be well approximated a polynomial of some low order p :

$$\mu^{(p)}(E) = \sum_{i=0}^p \mu_i E^i, \quad E = \omega - I. \quad (2)$$

We choose to optimize the fit over the entire range of excitation energies, not just about $E=0$ (the μ_i are simply related to the a , b , and c coefficients in Ref. 20). For example, the data in Fig. 3 can be accurately described by a straight line. We report the coefficients obtained through Eq. (2) in Table II and give the quantum defects obtained from these coefficients as continuous lines in Figs. 2 and 3. We also added the transition energies for He obtained from the KS fit to Table I. The maximum error in the fit is 3/100 mH so it is essentially exact for all purposes of this paper. We shall see that in other cases just two or even three coefficients are not enough to describe the data accurately. In those cases we will need to decide when to stop adding more coefficients to fit the data, since we would like to describe the data with as few coefficients as possible. Therefore we will look at the maximum absolute error in the quantum defect. By which we mean that

TABLE I. Transition energies for He atom (a.u.). The ionization energies are 0.903 724 4 a.u. for the singlet and triplet cases and 0.903 72 a.u. for the KS potential.

Transition	ΔE				Quantum defect		
	Singlet ^a	Triplet ^a	KS ^b	KS fit	Singlet	Triplet	KS
1s → 2s	0.757 750 3	0.728 494 9	0.745 99	0.745 96	0.149 252 5	0.310 798 2	0.219 57
1s → 3s	0.842 452 4	0.835 035 3	0.839 17	0.839 20	0.143 369 9	0.302 004 7	0.216 89
1s → 4s	0.870 137 6	0.867 212 2	0.868 83	0.868 82	0.141 653 5	0.299 446 4	0.214 92
1s → 5s	0.882 547 5	0.888 346 9	0.881 89	0.881 89	0.140 917 1	0.298 358 3	0.214 59
1s → 6s	0.889 161 3	0.892 594 4	0.888 79	0.888 79	0.140 533 0	0.297 795 4	0.214 41
1s → 7s	0.893 098 6	0.892 594 5	0.892 87	0.892 87	0.140 307 2	0.297 466 6	0.214 29

^aAccurate nonrelativistic calculations from Ref. 22.^bThe differences between the KS eigenvalues obtained with the exact potential from Ref. 23.

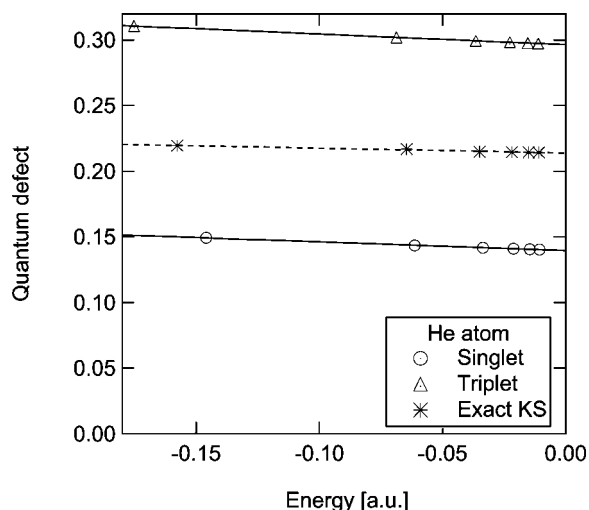


FIG. 3. Same as Fig. 2 plotted against energy.

we recalculate the quantum defects from the coefficients and look at the absolute differences between the fitted and original values and then look at the largest difference. We will stop adding more coefficients once the maximum absolute error is smaller than 0.001 or, in case this value is not reached, whenever the absolute errors do not change much when adding more coefficients. We give the value for the error also in Table II. Any approximate ground-state KS potential suggested for use in TDDFT should have its coefficients compared with the KS numbers in the table, while any approximate xc kernel should have its coefficients compared with the singlet and triplet cases.

III. GROUND-STATE KOHN-SHAM POTENTIALS

All linear response TDDFT calculations of excitations begin from the occupied to unoccupied transitions of the *ground-state* KS potential. In this section, we analyze some of the most popular approximations using quantum defect theory.

A. Computational details

All ground-state DFT results shown here are calculated with a modified optimized effective potential (OEP) model program.^{24–26} This program is basis set independent, works with a radial grid, and both the energies and the potentials are optimized in a self-consistent way. The exact-exchange (x-only) OEP is already included in this program. We also did calculations with the LB94 (Ref. 9) potential by Van Leeuwen and Baerends, which was not available in the pro-

TABLE II. Fit coefficients μ_0 and μ_1 for the *s* quantum defect of He. By “Max. AE” we mean the maximum absolute error as explained in the text.

	Singlet ^a	KS ^b	Triplet ^a
μ_0	0.1396	0.2139	0.2965
μ_1	-0.0655	-0.0370	-0.0811
Max. AE	0.0002	0.0006	0.0001

^aObtained from nonrelativistic calculations of the orbital energies from Ref. 22.

^bKS values obtained with the exact potential from Ref. 23.

TABLE III. The μ_i from the exact ground-state KS potential for He, Be, and Ne.

	He ^a	Be ^b	Ne ^b
		<i>s</i>	
I	0.9037	0.3426	0.7945
μ_0	0.2139	0.7164	1.3125
μ_1	-0.0370	-0.2785	-0.1807
Max. AE	0.0006	0.0002	0.0007
		<i>p</i>	
μ_0	0.0164	0.3587	0.8304
μ_1	0.0289	-0.3377	-0.3500
μ_2		0.6112	
Max. AE	0.0009	0.0003	0.001

^aReference 23.

^bReference 27.

gram. We implemented this functional by adding the LB94 correction to the LDA xc potential and let the program optimize this potential in a self-consistent manner. The program has the ability to read in the accurate potentials by Umrigar *et al.* [He,²³ Be,²⁷ and Ne (Ref. 27)]. The accurate potential of He was only known by us up to $r=20$. For technical reasons we needed to increase this radius to obtain energies for the higher n values. We did this by adding a $-1/r$ tail to v_{xc} and a Z/r tail to $v_{r\text{ mH}}$ and we checked that the transition was smooth. Since $r=20$ is far outside the density region of the atom, we do not expect this procedure to change the results within the reported accuracy. We also made sure that our values are converged with the number of grid points. When we used the accurate potentials, we did not allow the program to self-consistently change the potential.

The maximum n value for which we could still do very accurate calculations is $n=7$ for He and $n=9$ for Be and Ne.

B. Exact results

As we have seen the numbers μ_i contain all the information needed to characterize a given Rydberg series and make tables of the actual transition frequencies redundant. In Table III, we report the coefficients for *s* and *p* KS quantum defects for the He, Be, and Ne atoms obtained with accurate xc potentials. We use the transitions up to $n=9$ for the fit in case of Be and Ne and up to $n=7$ in case of He.

When we compare the *s* ($l=0$) values with *p* ($l=1$), the asymptotic KS quantum defect is smaller for *p* in all cases. This reflects the lesser importance of the inner part of the KS potential relative to the angular momentum barrier as l grows. However, the curvature of the *s* and *p* quantum defect is similar.

C. Approximations

In this section, we demonstrate our methodology by testing two common approximations for the ground-state KS potential. These are exact exchange OEP (Ref. 26) and LB94.⁹ Exact-exchange calculations are more demanding than traditional DFT calculations but are becoming popular because of the high quality of the potential.^{28,29} On the other hand, LB94 provides an asymptotically correct potential at

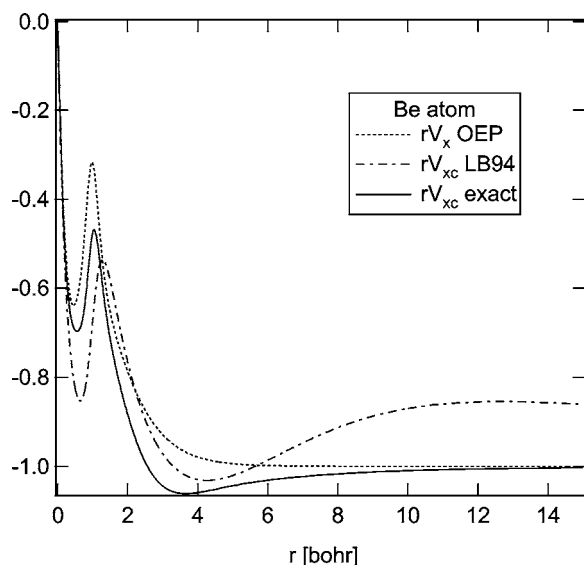


FIG. 4. The exact, LB94, and x-only potentials for beryllium together with $-1/r$.

little extra cost beyond traditional DFT.^{11,30,31} Figure 4 shows both of these potentials for the Be atom together with the exact potential.²⁷ Our figure for the exact potential is different from the one in Ref. 9, since in that reference they use a different accurate density to derive the potential. We give our values for the fit parameters in Table IV. In Fig. 5 we show the p Be quantum defect obtained with LB94, OEP, and KS and we show the fit as continuous lines. Figure 5 immediately shows the high quality of the OEP potential. The quantum defect curve is almost identical to the exact one, being offset by about 0.1 (see Table IV). On the other hand the quantum defect of LB94 is poor, and this is true for all cases

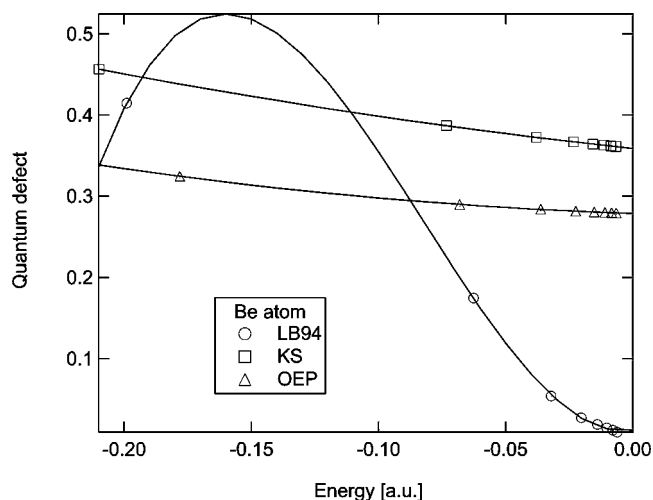


FIG. 5. The Be p quantum defect of LB94, OEP, and KS, and their best fits.

studied. From Fig. 4 we can see that the OEP is much closer to the true potential than LB94 and also approaches $-1/r$ faster. This shows that just having a potential that is asymptotically correct is not enough to get a good quantum defect.

Another thing we have not mentioned so far is that a potential that gives a wrong ionization potential does not necessarily give a bad quantum defect. The origin of this is that the quantum defect is obtained from $\omega_{nl} - I$ and can take a shift of energy levels into account. Consider the exact exchange results for the atoms. Typically, these quantum defects are accurate to 0.1. Thus, using the exact ionization potential with the exchange quantum defects yields highly accurate transition frequencies, i.e., the most significant error in OEP excitations is due to the missing correlation contribution to the position of the HOMO. On the other hand, we

TABLE IV. The μ_i from different ground-state potentials for He, Be, and Ne. The ionization energies are in a.u. and are not included in the maximum error.

		s			p		
		OEP	LB94	Exact	OEP	LB94	Exact
He	I	0.9182	0.8513	0.9037			
	μ_0	0.2170	-0.3607	0.2139	0.0238	-0.6015	0.0164
	μ_1	-0.0401	-2.7408	-0.0370	0.0319	-2.2013	0.0289
	μ_2		-3.1852			-1.5723	
	Max. AE	0.0000	0.003	0.0006	0.0000	0.002	0.0009
Be	I	0.3093	0.3205	0.3426			
	μ_0	0.6623	0.3497	0.7164	0.2786	0.0115	0.3287
	μ_1	-0.1557	-0.7203	-0.2785	-0.1070	0.4836	-0.3377
	μ_2		31.5313		0.8453	66.0517	0.6112
	μ_3		73.1572			268.6094	
Max. AE	0.0002	0.001	0.0002	0.0002	0.002	0.0003	
Ne	I	0.8508	0.7821	0.7945			
	μ_0	1.3433	0.8174	1.3125	0.8631	0.3196	0.8340
	μ_1	-0.2285	-3.2880	-0.1807	-0.3972	-2.8338	-0.3500
	μ_2		-11.0968			-1.3271	
	μ_3		-39.2359				
Max. AE	0.0004	0.004	0.0007	0.0008	0.003	0.001	

TABLE V. Transition energies for the beryllium atom.

Transition	Expt. ^a	KS ^b	ALDA ^c	Truncated ALDA ^d	Truncated hybrid ^e	WY ^f	AC-LDA ^g
$2s \rightarrow 3s$	0.249 13	0.244 37	0.2495	0.2515	0.2510	0.2512	0.2239
$2s \rightarrow 4s$	0.297 28	0.295 86	0.2977	0.2984	0.2985	0.3033	0.2680
$2s \rightarrow 5s$	0.315 86	0.315 26	0.3160	0.3164	0.3165		
$2s \rightarrow 6s$	0.324 96	0.324 66		0.3252	0.3254		
$2s \rightarrow 2p$	0.193 94	0.132 73	0.1868	0.1889	0.1427	0.1861	0.1781
$2s \rightarrow 3p$	0.274 23	0.269 37	0.2710	0.2714	0.2736	0.2749	0.2457
$2s \rightarrow 4p$	0.305 43	0.304 61	0.3048	0.3049	0.3059	0.3107	0.2754
$2s \rightarrow 5p$	0.319 49	0.319 31		0.3194	0.3199		
$2s \rightarrow 6p$	0.326 90	0.326 86		0.3269	0.3272		
s MAE (mH)			0.312	1.069	0.943	4.046	27.25
p MAE (mH)			3.669	1.700	10.61	4.592	24.81
Total MAE (mH)			1.991	1.420	6.313	4.374	25.79

^aExperimental values from NIST Ref. 38.

^bThe differences between the KS eigenvalues obtained with the exact potential from Ref. 27.

^cALDA calculation including all bound and unbound states from Ref. 33.

^dALDA calculation including 34 unbound states from Ref. 34.

^eHybrid calculation including 34 unbound states for He and 38 unbound states for Be from Ref. 35.

^fALDA calculation with WY ground-state potential from Ref. 39.

^gAsymptotically corrected ALDA results from Ref. 39.

see that LB94, while asymptotically correct and sometimes having a highly accurate ionization potential, has much less accurate quantum defects.

IV. TDDFT RESULTS

In the previous sections we saw that the KS quantum defects are typically lying in between the exact singlet and triplet quantum defects.³² In order to calculate these singlet and triplet quantum defects within DFT the usual method of choice is TDDFT (within the linear response regime). Apart from a ground-state potential one needs to choose an xc kernel as well. In this section we obtain quantum defects from excitation energies obtained with different xc kernels and ground-state potentials. We focus mainly on the Be atom, but we also give expansion coefficients for He and Ne quantum defects.

A. Performance of TDDFT

We concentrate on the quantum defect obtained from the adiabatic LDA (ALDA) kernel applied to the exact ground-state KS potential. In Table V, we show $s \rightarrow s$ and $s \rightarrow p$ excitation energies for the Be atom. The ALDA results in column 4 are obtained by van Gisbergen *et al.*³³ For their ground-state calculations, they used the accurate potential by Umrigar and Gonze²⁷ and for the xc kernel they used the ALDA. The calculations were done close to the basis set limit and with high numerical integration accuracy. As can be seen from the table the excitation energies for the $s \rightarrow s$ transitions are very close to the experimental values with a mean average error (MAE) of only 0.3 mH. The $s \rightarrow p$ excitation energies are a bit less accurate with an MAE of 3.7 mH, but this is still an accurate result. The fit coefficients for the quantum defects of these calculations are reported in Table VI. For the fit of the TDDFT results we took a less strict constraint to determine when to stop adding more coefficients. We took 0.01 instead of 0.001, reflecting the greater error in this data.

In Fig. 6 we show the s and p quantum defects corresponding to these values and we compare them with the bare KS and experimental results. For the s quantum defect, the experimental curve is essentially a straight line, with a small negative slope. The p quantum defect, on the other hand, is much more curved, with a large positive slope, due to the much lower $2s \rightarrow 2p$ transition. The exact KS potential has been touted as a good approximation to the experimental results.³² This is clearly true for the s curves but not so for the p quantum defect. In that case the KS quantum defect, while being very close to the experimental value as $n \rightarrow \infty$, has the wrong behavior as a function of E .

In both the s and p cases it is clear that doing a full TDDFT calculation considerably improves upon the bare KS results. The ALDA does slightly overcorrect the s quantum defect, underestimating the value at $E=0$. In case of the p quantum defect the ALDA tends to correct for the opposite slope of the KS values compared to the experimental values, but the correction is not complete, leading to a curved line. We also see that the s quantum defects as obtained with the ALDA are much better than the p quantum defects, even though the MAE is only a few millihenries in the last case.

B. Truncating Casida's equation

Another set of ALDA calculations were performed by Petersilka *et al.*³⁴ The difference between their calculation and that of van Gisbergen *et al.* is that they truncate the summation over states in the response function, including only poles of bound states and neglecting continuum contributions. They included the lowest 34 bound states of s and p symmetries in their calculations. Just like in the case of the full ALDA calculations the ground state was determined with the potential of Umrigar and Gonze.²⁷ We show these results in column 5 of Table V. Again the results are close to the experimental values with a MAE of 1.1 mH for the $s \rightarrow s$ transitions and a MAE of 1.7 mH for the $s \rightarrow p$ transitions. In Fig. 7 we show the s and p quantum defects corresponding to

TABLE VI. The μ_i from different singlet TDDFT values for Be.

	Reference ^a	KS ^b	ALDA ^c	Truncated ALDA ^d	Truncated hybrid ^e	WY/ALDA ^f	AC-LDA ^g
<i>s</i>							
<i>I</i>	0.3426	0.3426	0.3426	0.3426	0.3426	0.3493	0.3111
μ_0	0.6752	0.7164	0.6536	0.6182	0.6010	0.6684	0.5997
μ_1	-0.0133	-0.2785	-0.2986	-0.4294	-0.6947	-0.7540	
μ_2	1.2345						
Max. AE	0.0003	0.0002	0.004	0.002	0.004	0.0000	0.006
<i>p</i>							
μ_0	0.3745	0.3287	0.3327	0.3427	0.3087	0.3484	0.2413
μ_1	1.1612	-0.3377	-1.3172	-0.9634	0.2505	-1.9702	-1.1215
μ_2	1.5678	0.6112	-13.5673	-12.4534	3.9961	-15.7792	-18.6196
μ_3	21.4587						
Max. AE	0.0002	0.0003	0.0000	0.003	0.004	0.0000	0.0000

^aExperimental values from NIST Ref. 38.^bThe differences between the KS eigenvalues obtained with the exact potential from Ref. 27.^cALDA calculation including all bound and unbound states from Ref. 33.^dALDA calculation including 34 unbound states from Ref. 34.^eHybrid calculation including 38 unbound states from Ref. 35.^fALDA calculation with WY ground-state potential from Ref. 39.^gAsymptotically corrected ALDA results from Ref. 39.

these values and we compare them with the full ALDA results. For the *s* quantum defect we see that the quantum defect is slightly below the ALDA values, and the slope is too large, leading to a smaller asymptotic quantum defect. For the *p* quantum defect we see that there is not much difference between the truncated and the full results. So the effect of the truncation in case of Be is not so great. For He the difference is relatively larger, because the TDDFT corrections are so small. This can be seen from the values in Tables VI and VII, which we will discuss in Sec. IV F.

C. Quality of the ground-state potential

For all TDDFT methods we have described so far, the ground state was calculated with the exact potential of Umrigar and Gonze.²⁷ This eliminates errors in the ground state so one can compare the effects of using a different xc kernel.

But for practical calculations such an accurate potential is not available. This motivates the development of other accurate ground-state potentials to calculate the Rydberg series.

Wu and Yang¹² (WY) obtained an accurate potential by a direct optimization method that allows them to calculate the potential from a given electronic density. This density is obtained from a coupled-cluster singles and doubles (CCSD) calculation. In Table V we show the excitation energies corresponding to the WY potentials and the error is just a few millihenries. In Fig. 8 we show the quantum defects obtained with this potential and compare them with the ALDA and experimental values. Only the asymptotic value of the quantum defect is accurate. Errors due to (very small) errors in the ground-state density are visible for all other energies and can be comparable to the xc kernel itself. The WY method is therefore still very promising but clearly requires a very accurate input density. Quantum defect analysis should prove

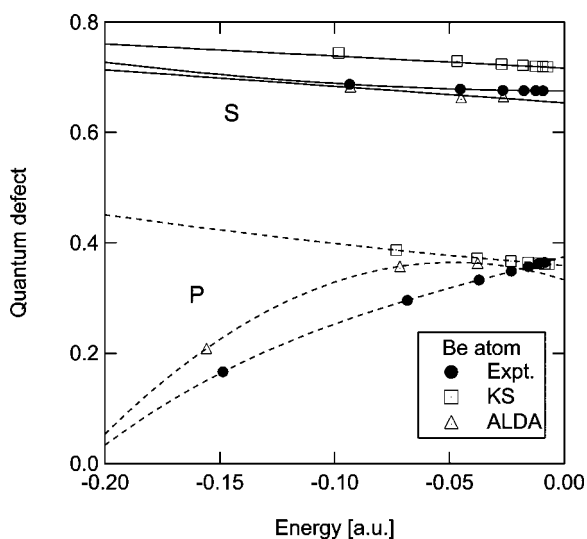
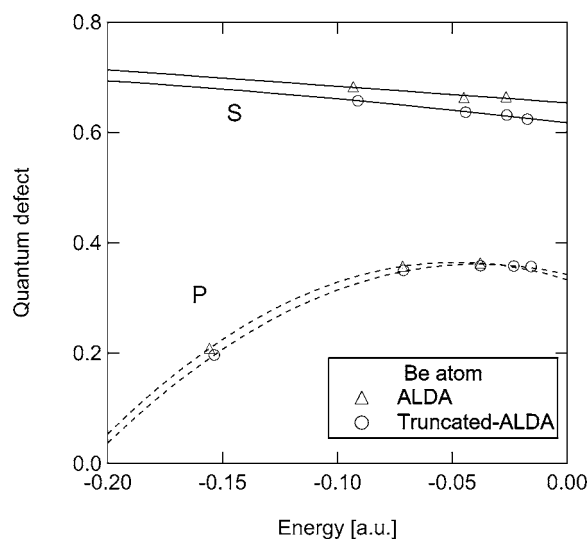
FIG. 6. The *s* and *p* experimental, KS, and ALDA singlet quantum defects for Be. The continuous lines are the $\mu^{(p)}(E)$ fits.FIG. 7. The *s* and *p* ALDA and truncated-ALDA singlet quantum defects for Be. The continuous lines are the $\mu^{(p)}(E)$ fits.

TABLE VII. The μ_i from different singlet TDDFT values for He.

	Reference ^a	KS ^b	ALDA ^c	Truncated ALDA ^d	Truncated hybrid ^e	WY/ALDA ^f	AC-LDA ^g
<i>s</i>							
<i>I</i>	0.9037	0.9037	0.9037	0.9037	0.9037	0.9026	0.7817
μ_0	0.1395	0.2139	0.1099	0.0223	0.0599	0.0226	-0.1027
μ_1	-0.0655	-0.0370	-0.1388	-0.4537	-0.5390	-2.4879	-4.3920
μ_2					-12.6664	-25.7710	
Max. AE	0.0002	0.0006	0.001	0.006	0.007	0.03	0.06
<i>p</i>							
μ_0	-0.0122	0.0164	-0.0002	-0.0168	-0.0355	-0.1039	-0.1579
μ_1	-0.0227	0.0289	-0.2077	-0.2721	-0.2201	-6.1973	-2.0656
μ_2					-107.6068	-13.2488	
μ_3					-521.8636		
Max. AE	0.0001	0.0009	0.005	0.002	0.008	0.007	0.02

^aNonrelativistic calculations from Ref. 22.^bThe differences between the KS eigenvalues obtained with the exact potential of Ref. 23.^cALDA calculation including all bound and unbound states from Ref. 33.^dALDA calculation including 34 unbound states from Ref. 34.^eHybrid calculation including 34 unbound states from Ref. 35.^fALDA calculation with WY ground-state potential from Ref. 39.^gAsymptotically corrected ALDA results from Ref. 39.

very useful for testing WY-type calculations, for example, for comparing basis set errors with errors due to the level of calculation used for obtaining the input density.

D. Testing approximate kernels

In an attempt to improve the xc kernel, Burke *et al.*³⁵ suggested the following form:

$$f_{xc}^{\uparrow\uparrow} = f_x^{\uparrow\uparrow}, \quad f_{xc}^{\uparrow\downarrow} = f_{xc}^{\uparrow\downarrow ALDA}. \quad (3)$$

This form is based on the fact that the parallel-spin contribution is well described in the exact exchange case because of a cancellation of exchange contributions. But an exact exchange treatment misses the significant antiparallel correlation contribution, leading to too large singlet/triplet splittings. Therefore it is recommended that for the antiparallel kernel one uses the ALDA. We show the excitation energies

obtained with this kernel in Table V. It should be noted that just as in the case of the truncated-ALDA calculations, the number of states included in the hybrid calculation is also limited. Namely, 34 states in case of He and 38 states in case of Be. Therefore we shall denote the method by truncated hybrid. The ground state of these calculations was again calculated with the exact potential of Umrigar and Gonze.²⁷ Apart from the $2s \rightarrow 2p$ transition the truncated-hybrid results are very similar to the truncated-ALDA results. It is the large error in the $2s \rightarrow 2p$ transition that leads to the large MAE.

In Fig. 9 we show the *s* and *p* quantum defects corresponding to the truncated-hybrid results and we compare them with the truncated-ALDA and experimental results. From the *s* quantum defect plot, it can again be seen that the truncated-hybrid results are close to the truncated-ALDA values, so the kernel does not improve the results in this case.

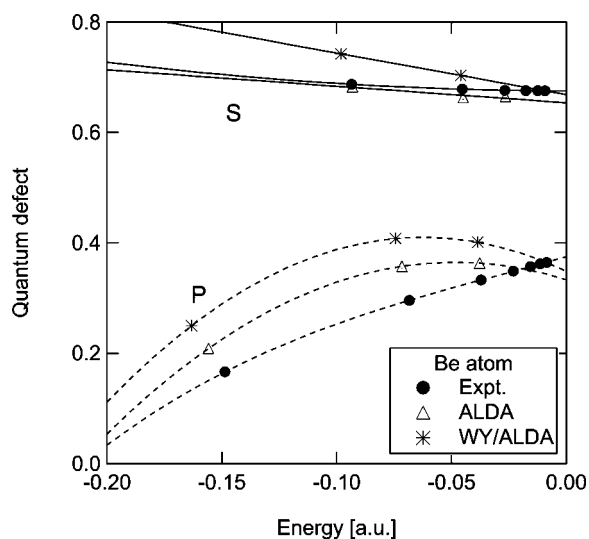


FIG. 8. The *s* and *p* experimental, ALDA, and WY quantum defects for Be. The continuous lines are the $\mu^{(p)}(E)$ fits.

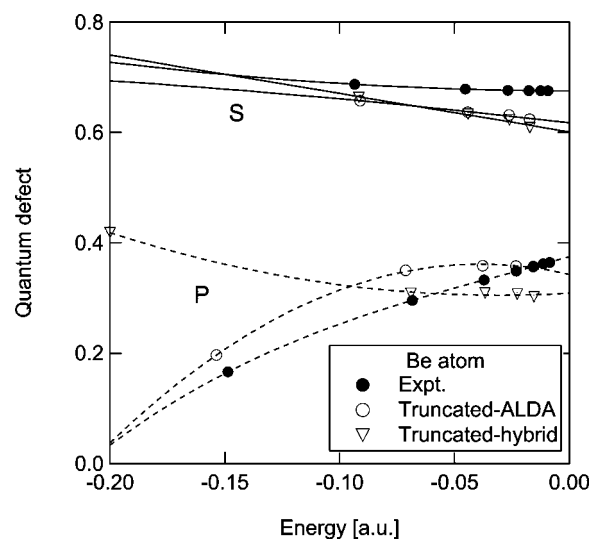


FIG. 9. The *s* and *p* experimental, truncated-ALDA, and truncated-hybrid singlet quantum defects for Be. The continuous lines are the $\mu^{(p)}(E)$ fits.

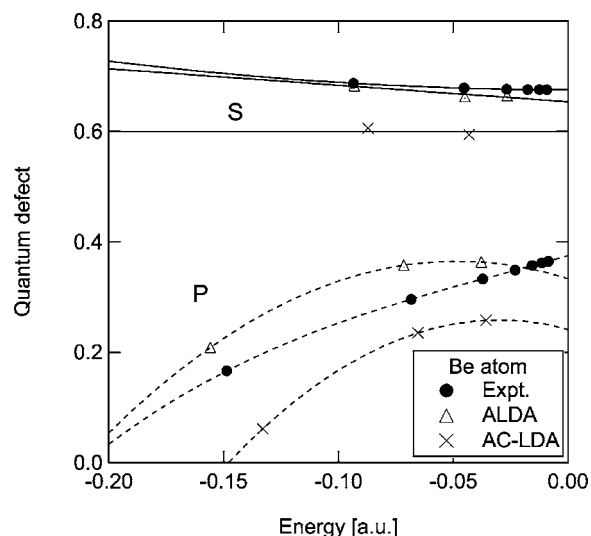


FIG. 10. The s and p experimental, ALDA, and AC-LDA quantum defects for Be. The continuous lines are the $\mu^{(p)}(E)$ fits.

For the p quantum defect, the results actually get worse with the truncated hybrid giving a slope opposite the experimental curve, so it shifts the KS values in the right direction but does not correct for the wrong slope. The hybrid kernel does not improve much upon the truncated ALDA for Be as was also found in Ref. 35. It is only good for two-electron systems, for which it was derived.

E. Asymptotically corrected ground-state potentials

Wu *et al.*³¹ obtained an asymptotically corrected LDA (AC-LDA) potential by a variational method that forces the potential to have the correct asymptotic behavior. This is a pure DFT treatment that can be applied to larger molecules. We see from Table V that the AC-LDA gives a large MAE.

In Fig. 10 we show the quantum defects obtained with the AC-LDA potential and compare them with the KS and

experimental values. In both cases the AC-LDA values are much lower than the ALDA, which was evaluated on the exact ground-state KS potential. The AC-LDA strongly underestimates the experimental s and p quantum defects. The shape of the p curve is similar to the ALDA curve. From this figure, it is clear that there are significant errors in the underlying KS potential.

F. Coefficients for He

In this section we give the values of the best fit for He as defined in Eq. (2) and as described thereafter. The original excitation energies from which the quantum defects and corresponding coefficients are calculated are obtained from the same sources as the Be data described above. In Table VII, we give the results for He. The sizes of the quantum defects are much smaller than in Be, and the fractional change between KS and experiment is concomitantly larger. In the case of the p quantum defects, they can have large opposite signs. Application of ALDA to the exact ground-state KS potential again works well.

In the case of He, the truncated-hybrid result improves upon the truncated ALDA. As we mentioned before this is because the hybrid was developed for two-electron systems. AC-LDA and WY coefficients of He really stand out as behaving much differently from the other cases and giving large errors that cannot be removed by adding more coefficients. The AC-LDA and WY coefficients of Be did not have this problem.

G. Triplets

In practice, spin decomposed TDDFT is commonly used and allows prediction of singlet \rightarrow triplet transitions. In this section we discuss the coefficients of the quantum defect expansion obtained from triplet excitation energies. In Table VIII we show the fit coefficients for He and Be. For the WY and AC-LDA methods there are no triplet data available. For

TABLE VIII. The μ_i from different triplet TDDFT values for He and Be.

		Reference ^a	ALDA ^b	Truncated ALDA ^c	Truncated hybrid ^d
		s			
He	μ_0	0.2965	0.2719	0.2570	0.317 1
	μ_1	-0.0811	-0.0892	-0.1281	
	Max. AE	0.0001	0.004	0.003	0.007
Be	μ_0	0.7742	0.7706	0.7641	0.768 3
	μ_1	0.8870	-0.3912	-0.4015	-0.260 7
	Max. AE	0.001	0.0003	0.002	0.002
		p			
He	μ_0	0.0684	0.0734	0.0657	0.053 32
	μ_1	0.0457			0.110 3
	Max. AE	0.0002	0.003	0.005	0.002
Be	μ_0	0.3620	0.4152	0.4101	0.378 52
	μ_1	-0.4492	0.3553	-0.7166	-0.640 4
	μ_2	1.5829			1.522 5
	Max. AE	0.0003	0.004	0.006	0.007

^aHe nonrelativistic calculations from Ref. 22 and Be and Ne experimental values from NIST (Ref. 38).

^bALDA calculation including all bound and unbound states from Ref. 33.

^cALDA calculation including 34 unbound states from Ref. 34.

^dHybrid calculation including 34 unbound states for He and 38 unbound states for Be from Ref. 35.

the triplet case, the μ_0 's are very well reproduced in all cases; also other coefficients are often close. Overall the data can in most cases be reproduced by only two or three coefficients.

V. CONCLUSIONS

We have shown that a plot of the quantum defect can be more insightful than a list of excitation energies, when reporting Rydberg states obtained with DFT. The quantum defect can also be fitted to an expansion around $E=0$ and a finite number of expansion coefficients can fully describe the Rydberg series. We note that although the perturbation theory of Drake and Swainson³⁶ also relates the asymptotic behavior of a long-ranged potential to its quantum defect, it does not apply here because it requires l to be large.

We calculated the quantum defects for He, Be, and Ne with accurate xc potentials and showed that the KS quantum defect lies between the interacting singlet and triplet values. We also studied approximate asymptotically corrected ground-state KS potentials, namely, the LB94 and OEP potentials. We saw that the OEP results are very close to the exact KS values. The LB94 underestimates the quantum defect in all cases. Again the data can be fully described by a few coefficients.

In the final part of the paper we calculated the quantum defects from available TDDFT excitation energies from the literature. We see that the quantum defect really amplifies the error in these cases. The TDDFT data can be described by only a few coefficients.

Overall we see that while having an asymptotically corrected potential guarantees the existence of a Rydberg series, it is not necessarily a good one. This is especially the case for AC-LDA TDDFT and LB94 ground-state values and to a lesser extent even for the WY TDDFT values.

Finally, we want to point out that the recent work of Wasserman and Burke³⁷ shows how to extract $\mu(E=0)$ from *short-ranged* potentials. Our analysis here will provide a useful tool for further development of that method.

ACKNOWLEDGMENTS

We thank Qin Wu for providing the ionization energies corresponding to their AC-LDA and WY calculations. We also thank Robert van Leeuwen for useful discussions. This work was supported by NSF Grant No. CHE-0355405.

- ¹E. Runge and E. K. Gross, Phys. Rev. Lett. **52**, 997 (1984).
- ²F. Furche and D. Rappoport, in *Computational Photochemistry*, edited by M. Olivucci (Elsevier, Amsterdam, to be published).
- ³K. Burke, J. Werschnik, and E. K. U. Gross, J. Chem. Phys. **123**, 062206 (2005).
- ⁴M. van Faassen and P. L. de Boeij, J. Chem. Phys. **120**, 8353 (2004).
- ⁵M. Petersilka, U. J. Gossmann, and E. K. U. Gross, Phys. Rev. Lett. **76**, 1212 (1996).
- ⁶M. Levy, J. P. Perdew, and V. Sahni, Phys. Rev. A **30**, 2745 (1984).
- ⁷C. O. Almbladh and A. C. Pedroza, Phys. Rev. A **29**, 2322 (1984).
- ⁸A. Mattsson, Science **298**, 5594 (2002).
- ⁹R. van Leeuwen and E. J. Baerends, Phys. Rev. A **49**, 2421 (1994).
- ¹⁰D. J. Tozer and N. C. Handy, J. Chem. Phys. **109**, 10180 (1998).
- ¹¹M. E. Casida and D. R. Salahub, J. Chem. Phys. **113**, 8918 (2000).
- ¹²Q. Wu and W. Yang, J. Chem. Phys. **118**, 2498 (2003).
- ¹³H. Friedrich, *Theoretical Atomic Physics*, 2nd ed. (Springer-Verlag, Berlin, 1998).
- ¹⁴M. J. Seaton, Rep. Prog. Phys. **46**, 167 (1983).
- ¹⁵M. Aymar, C. H. Greene, and E. Luc-Koenig, Rev. Mod. Phys. **68**, 1015 (1996).
- ¹⁶G. Herzberg, Annu. Rev. Phys. Chem. **38**, 27 (1987).
- ¹⁷I. D. Petsalakis, G. Theodorakopoulos, and R. J. Buenker, J. Chem. Phys. **119**, 2004 (2003).
- ¹⁸R. Guérout, M. Jungen, and C. Jungen, J. Phys. B **37**, 3043 (2004).
- ¹⁹R. Guérout, M. Jungen, and C. Jungen, J. Phys. B **37**, 3057 (2004).
- ²⁰A. I. Al-Sharif, R. Resta, and C. J. Umrigar, Phys. Rev. A **57**, 2466 (1998).
- ²¹M. J. Seaton, Mon. Not. R. Astron. Soc. **188**, 504 (1955).
- ²²G. W. F. Drake, in *Atomic, Molecular, and Optical Physics Handbook*, edited by G. W. F. Drake (AIP, Woodbury, NY, 1996), p. 154.
- ²³C. J. Umrigar and X. Gonze, Phys. Rev. A **50**, 3827 (1994).
- ²⁴E. Engel, (private communication).
- ²⁵E. Engel and R. M. Dreizler, J. Comput. Chem. **20**, 31 (1999).
- ²⁶J. D. Talman and W. G. Shadwick, Phys. Rev. A **14**, 36 (1976).
- ²⁷C. J. Umrigar and X. Gonze, in *High Performance Computing and its Application to the Physical Sciences*, edited by D. A. Browne, J. Callaway, J. P. Draayer, R. W. Haymaker, R. K. Kalia, J. E. Tohlne, P. Vashishta (World Scientific, Singapore, 1993), Vol. 94.
- ²⁸A. Görling, Phys. Rev. Lett. **83**, 5459 (1999).
- ²⁹S. Ivanov, S. Hirata, and J. Bartlett, Phys. Rev. Lett. **83**, 5455 (1999).
- ³⁰M. Grüning, O. V. Gritsenko, S. J. A. van Gisbergen, and E. J. Baerends, J. Chem. Phys. **112**, 652 (2001).
- ³¹Q. Wu, P. W. Ayers, and W. Yang, J. Chem. Phys. **119**, 2978 (2003).
- ³²A. Savin, C. J. Umrigar, and X. Gonze, Chem. Phys. Lett. **288**, 391 (1998).
- ³³S. J. A. van Gisbergen, F. Kootstra, P. R. T. Schipper, O. V. Gritsenko, J. G. Snijders, and E. J. Baerends, Phys. Rev. A **57**, 2556 (1998).
- ³⁴M. Petersilka, E. K. U. Gross, and K. Burke, Int. J. Quantum Chem. **80**, 534 (2000).
- ³⁵K. Burke, M. Petersilka, and E. K. U. Gross, in *Recent Advances in Density Functional Methods*, edited by V. Barone, P. Fantucci, and A. Bencini (World Scientific, Singapore, 2000), Vol. 3, pp. 67–79.
- ³⁶G. W. F. Drake and R. A. Swainson, Phys. Rev. A **44**, 5448 (1991).
- ³⁷A. Wasserman and K. Burke, Phys. Rev. Lett. **95**, 163006 (2005).
- ³⁸NIST Atomic Spectra Database, <http://physics.nist.gov/PhysRefData/ASD/index.html>
- ³⁹Q. Wu, A. J. Cohen, and W. Yang, Mol. Phys. **103**, 711 (2005).